CALCULATING THE NONSTEADY EXCHANGE OF MASS AND HEAT IN THE LAMINAR FLOW OF DISSOCIATING NITROGEN TETRAOXIDE IN A FUEL-CELL CLUSTER

V. V. Lapin and A. A. Ryadno

UDC 536.24

We propose a method for the numerical calculation of the nonsteady exchange of mass and heat in the flow of a chemically reactive coolant in channels of complex shape. As an example we present the results from the calculations of heat and mass exchange in the laminar flow of dissociating N_2O_4 for a triangular fuel-cell cluster.

The study of the processes involved in convective heat and mass exchange in the flow of chemically reactive gases in channels is made markedly more difficult by nonlinearities resulting from the presence of chemical sources of mass and heat, the dependence of thermophysical and coolant transport properties on temperature, pressure, and the composition of the mixture, the complex nature of the chemical interactions, the processes of diffusion, and on the heat conduction and hydrodynamics of the flow [1].

The majority of publications at the present time are devoted to the results of theoretical [1] and experimental [2] studies into stationary heat and mass exchange. The numerical studies are associated primarily with the application of the method of finite differences (MFD) [1, 3] and the method of finite elements (MFE) [4, 5]. The unique features of nonsteady heat and mass exchange processes for such flows have not yet been studied adequately. The article [6] is devoted to experimental studies of nonsteady flows of dissociating N_2O_4 coolant.

The present paper gives results from numerical investigations into the nonstationary transfer of heat and mass in the longitudinal streamlining of fuel-cell clusters by a laminar flow of dissociating nitrogen tetroxide.

Let us examine a model of the active zone of a nuclear reactor, which is formed by a bundle of heat-releasing rods surrounded by a noncatalytic shell, these rods positioned in a checkerboard array and streamlined with a longitudinal flow of dissociating N_2O_4 (Fig. 1). Let us take into consideration the simultaneous occurrence of the I and II stages of the dissociation, i.e., the equilibrium stage $N_2O_4 \leftrightarrows 2NO_2$ and the essentially nonequilibrium stage $2NO_2 \leftrightarrows 2NO + O_2$, assuming that the "frozen in" components of the thermophysical and transport properties of the mixture are constant. Since the nitrogen oxide and the molecular oxygen exhibit similar molecular weights and parameters of intermolecular interaction, they exhibit virtually no diffusion separation within the flow, i.e., the stoichiometric relationship is maintained between the concentrations of the components NO and O_2: $C_3 = 2m_3C_4/m_4$.

The velocity profile in the hydrodynamically stabilized stationary laminar flow is determined from the solution of the Poisson equation

$$\frac{\partial^2\omega_z}{\partial x^2} + \frac{\partial^2\omega_z}{\partial y^2} = -\frac{\Delta P}{\mu l} \qquad (1)$$

with boundary conditions of adhesion at the streamlined surface and conditions of impermeability on the symmetry lines which form the contours of the region for which these calculations are being carried out.

Let us present a system of equations to describe the nonstationary conjugate heat and mass exchange for this flow, a system constructed with provision for generally accepted as-

Dnepropetrovsk Metallurgy Institute. Dnepropetrovsk State University. Translated from Inzhenerno-Fizicheskii Zhurnal, Vol. 57, No. 4, pp. 658-667, October, 1989. Original article submitted March 22, 1988.

0022-0841/89/5704-1245$12.50

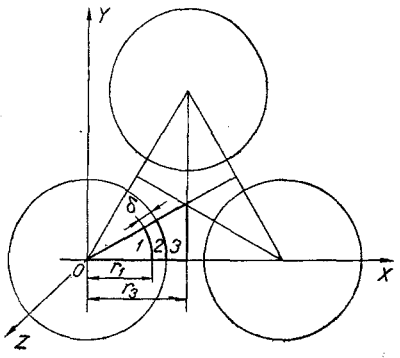

Fig. 1. Area of design: 1) fuel core Ω_a; 2) fuel cell shell Ω_b; 3) coolant flow region Ω_c. Relative fuel-cell grid spacing $\beta = r_3/(r_1 + \delta)$.

sumptions [7], in particular, the assumption that the transfer of heat and mass along the axis of the channel, as a result of heat conduction and diffusion, is small in comparison with convective heat and mass transfer.

The equation of energy conservation in the flow region:

$$(c_{pf} + c_{pr})\rho\frac{\partial T}{\partial \tau} + (c_{pf} + c_{pr})\rho\omega_z\frac{\partial T}{\partial z} = \frac{\partial}{\partial x}\left((\lambda_f + c_{pr}\rho D_1)\frac{\partial T}{\partial x}\right) + \frac{\partial}{\partial y}\left((\lambda_f + c_{pr}\rho D_1)\frac{\partial T}{\partial y}\right) - (\Delta H_{pI}\varphi_1 + \Delta H_{pII})\frac{J_4}{m_4}. \quad (2)$$

The equations of heat conduction in the shell and in the fuel core of the fuel cell, without taking into consideration the axial component, owing to the great length of the fuel assembly and the limited diameter of the rods are as follows:

$$c_{pb}\rho_b\frac{\partial T_b}{\partial \tau} = \lambda_b\left(\frac{\partial^2 T_b}{\partial x^2} + \frac{\partial^2 T_b}{\partial y^2}\right), \quad (3)$$

$$c_{pc}\rho_c\frac{\partial T_c}{\partial \tau} = \lambda_c\left(\frac{\partial^2 T_c}{\partial x^2} + \frac{\partial^2 T_c}{\partial y^2}\right) + q_v(\tau). \quad (4)$$

The equation for the conservation of the oxygen mass is

$$\rho D_4\frac{\partial C_4}{\partial \tau} + \rho D_4\omega_z\frac{\partial C_4}{\partial z} = \rho D_4\left(\frac{\partial^2 C_4}{\partial x^2} + \frac{\partial^2 C_4}{\partial y^2}\right) + J_4. \quad (5)$$

Equations (1) and (5) are enhanced by means of the following relationships [1]:

$$J_4 = m_4 K_{npII}\left(\left(\frac{\rho C_2}{m_2}\right)^2 - \frac{4}{K_{cII}}\left(\frac{\rho C_4}{m_4}\right)^3\right),$$

$$c_{pr} = \frac{\Delta H_{pI}^2}{m_1 RT^2\left(\frac{1}{C_1} + \frac{2}{C_2} - \frac{m}{m_1}\right)},$$

$$\varphi_1 = \frac{\frac{2}{C_1} + \frac{m}{m_1}}{\frac{1}{C_1} + \frac{2}{C_2} - \frac{m}{m_1}},$$

$$m = \left(\frac{2}{m_1} - \frac{C_1}{m_1} + \frac{C_4}{m_4}\right)^{-1}.$$

The concentrations of NO_2 and N_2O_4 are determined from the following formulas, respectively:

$$C_2 = 1 - C_1 - \frac{m_1 C_4}{m_4}, \quad C_1 = \frac{m_1\rho}{K_{cI}}\left(\frac{C_2}{m_2}\right)^2.$$

The latter relationship follows from the condition of equilibrium for stage I of the nitrogen tetroxide dissociation reaction.

The thermophysical and transport properties of the mixture and the velocity and equilibrium constants of the reactions are calculated on the basis of relationships found in [1, 7].

At the initial instant of time and at the inlet to the channel we have specified constant temperature T_0 and concentration C_{40} profiles. We required a condition of thermal insulation at the symmetry lines bounding the calculation region, and conditions of conjugacy between the temperatures and heat flows at the boundaries of media separation, i.e., between the core and the shell and between the shell and the coolant. For the equation of mass transport (5) we impose the condition of equality to zero for the normal derivative at the boundary of the flow region.

System of equations (1)-(5) in dimensionless form has the following form:

$$\frac{\partial^2 W}{\partial X^2}+\frac{\partial^2 W}{\partial Y^2}=-32K_\Phi, \tag{6}$$

$$K_{cpa}(1+\Phi)\frac{\partial\Theta_a}{\partial \mathrm{Fo}}+K_{\lambda a}\mathrm{Pe}\,W(1+\Phi)\frac{\partial\Theta_a}{\partial Z}=$$
$$=K_{\lambda a}\left(\frac{\partial}{\partial X}\left((1+\Phi\,\mathrm{Le}_1)\frac{\partial\Theta_a}{\partial X}\right)+\frac{\partial}{\partial Y}\left((1+\Phi\,\mathrm{Le}_1)\frac{\partial\Theta_a}{\partial Y}\right)\right)-Q_a', \tag{7}$$

$$K_{cpb}\frac{\partial\Theta_b}{\partial \mathrm{Fo}}=K_{\lambda b}\left(\frac{\partial^2\Theta_b}{\partial X^2}+\frac{\partial^2\Theta_b}{\partial Y^2}\right), \tag{8}$$

$$K_{cpc}\frac{\partial\Theta_c}{\partial \mathrm{Fo}}=K_{\lambda c}\left(\frac{\partial^2\Theta_c}{\partial X^2}+\frac{\partial^2\Theta_c}{\partial Y^2}\right)+Q_c, \tag{9}$$

$$K_{cpa}\frac{\partial C}{\partial \mathrm{Fo}}+K_{\lambda a}\mathrm{Pe}\,W\frac{\partial C}{\partial Z}=K_{\lambda a}\mathrm{Le}_i\left(\frac{\partial^2 C}{\partial X^2}+\frac{\partial^2 C}{\partial Y^2}\right)+Q_a''. \tag{10}$$

Since the hydrodynamic problem is independent of the heat and mass exchange problem, the equation of motion and the equations of heat and mass transport can be solved separately.

To solve the system of equations (6)-(10) with the described initial and boundary conditions we make use both of the MFE and MFD methods, the former for the approximation of the sought functions from the coordinates of the lateral cross section of the channel, and the latter for the approximation of the time derivatives and the axial transport terms.

The region for which these calculations are being carried out is separated into m triangular simplex elements with three nodes in each, for a total of n nodes. The coolant flow region has m_2 elements and n_2 nodes, and the fuel-cell region has m_1 and n_1 elements, respectively, with $m = m_1 + m_2$ and $n = n_1 + n_2$. For purposes of interpolating the velocity, temperature, and concentration for these elements we select linear basis functions (form functions) [N]. These functions are represented in the form:

$$W(X, Y)=[N]\{\omega^{(k)}\},$$
$$\Theta(X, Y, Z, \mathrm{Fo})=[N]\{\vartheta^{(k)}\},$$
$$C(X, Y, Z, \mathrm{Fo})=[N]\{c^{(k)}\},$$

where $\{\omega^{(k)}\}$, $\{\vartheta^{(k)}\}$, and $\{c^{(k)}\}$ represent the values of the velocity, the temperature, and the concentration, respectively, at the nodes of the δ_k element.

Following the procedure of the Bubnov–Galerkin method, we will require satisfaction of the condition of orthogonality for the discrepancies which arise on substitution into the original equations of the interpolation expressions for W, Θ, and C, to the basis functions:

$$\int_{\delta_k}[N]^T\left(\frac{\partial^2 W}{\partial X^2}+\frac{\partial^2 W}{\partial Y^2}+32K_\Phi\right)d\delta_k=0, \tag{11}$$

$$\int_{\delta_k}[N]^T\left(K_{\lambda a}\left(\frac{\partial}{\partial X}\left((1+\Phi\,\mathrm{Le}_1)\frac{\partial\Theta_a}{\partial X}\right)+\frac{\partial}{\partial Y}\left((1+\Phi\,\mathrm{Le}_1)\frac{\partial\Theta_a}{\partial Y}\right)\right)-\right. \tag{12}$$

$$-Q_a'-K_{c\rho a}(1+\Phi)\frac{\partial\Theta_a}{\partial \mathrm{Fo}}-K_{\lambda a}\,\mathrm{Pe}\,W(1+\Phi)\frac{\partial\Theta_a}{\partial Z}\Big)\,d\delta_k=0,$$

$$\int_{\delta_k}[N]^T\left(K_{\lambda b}\left(\frac{\partial^2\Theta_b}{\partial X^2}+\frac{\partial^2\Theta_b}{\partial Y^2}\right)-K_{c\rho b}\frac{\partial\Theta_b}{\partial \mathrm{Fo}}\right)d\delta_k=0, \tag{13}$$

$$\int_{\delta_k}[N]^T\left(K_{\lambda c}\left(\frac{\partial^2\Theta_c}{\partial X^2}+\frac{\partial^2\Theta_c}{\partial Y^2}\right)+Q_c-K_{c\rho c}\frac{\partial\Theta_c}{\partial \mathrm{Fo}}\right)d\delta_k=0, \tag{14}$$

$$\int_{\delta_k}[N]^T\left(K_{\lambda a}\,\mathrm{Le}_i\left(\frac{\partial^2 C}{\partial X^2}+\frac{\partial^2 C}{\partial Y^2}\right)+Q_a''-\right. \tag{15}$$

$$\left.-K_{c\rho a}\frac{\partial C}{\partial \mathrm{Fo}}-K_{\lambda a}\,\mathrm{Pe}\,W\frac{\partial C}{\partial Z}\right)d\delta_k=0.$$

Equations (11), (12), and (15) have been determined in the flow region, while Eq. (13) has been determined for the shell, and Eq. (14) in the region of the core.

Applying the Ostrogradskii–Gauss formula and summing expression (11) over all elements of the coolant flow region, we obtain a system of linear algebraic equations for the velocity values at the nodes:

$$[D]\{\omega\}=\{F\}. \tag{16}$$

Here [D] is a quadratic matrix with dimensions of $n_2 \times n_2$ and elements

$$[\alpha_{ij}]=\Sigma\int_{\delta_k}\left(\frac{\partial[N]^T}{\partial X}\frac{\partial[N]}{\partial X}+\frac{\partial[N]^T}{\partial Y}\frac{\partial[N]}{\partial Y}\right)d\delta_k,$$

{F} is a vector of length n_2 with the components

$$\{f_i\}=-32K_\Phi\Sigma\int_{\delta_k}[N]^T\,d\delta_k.$$

After modification of matrix [D], associated with the realization of the boundary condition of adhesion for velocity at the surface of the shell (the symmetry condition $\partial W/\partial n = 0$ on application of the Bubnov–Galerkin method is satisfied automatically), system (16) is solved by the Gaussian elimination method.

In analogous fashion, summing expression (12) over the elements of the flow region, expression (13) over the shell, and expression (14) over the fuel core, and expression (15) over the elements of the flow region, we obtain a system of partial differential equations of the hyperbolic type relative to the temperature values at the nodes of the entire calculation region and relative to the concentration values at the nodes of the flow region:

$$[A_1]\frac{\partial\{\vartheta\}}{\partial \mathrm{Fo}}+[B_1]\frac{\partial\{\vartheta\}}{\partial Z}=[R_1]\{\vartheta\}+\{G_1\}, \tag{17}$$

$$[A_2]\frac{\partial\{c\}}{\partial \mathrm{Fo}}+[B_2]\frac{\partial\{c\}}{\partial Z}=[R_2]\{c\}+\{G_2\}. \tag{18}$$

Here $[A_1]$, $[B_1]$, $[R_1]$ and $[A_2]$, $[B_2]$, $[R_2]$ represent quadratic matrices of dimension $n \times n$ and $n_2 \times n_2$, respectively, and $\{G_1\}$ and $\{G_2\}$ are vectors of length n and n_2. The elements of the matrix and of the vectors are determined from the formulas

$$[a_{ij}]=\begin{cases}K_{c\rho}\Sigma\int_{\delta_k}[N]^T[N]\,d\delta_k, & X,\ Y\in\Omega_c\cup\Omega_b,\\ K_{c\rho a}\Sigma\int_{\delta_k}[N]^T[N](1+\{\Phi^{(k)}\}[N])\,d\delta_k, & X,\ Y\in\Omega_a,\end{cases}$$

$$[b_{ij}]=\Big\{0,\ X,\ Y\in\Omega_c\cup\Omega_b,\ K_{\lambda a}\,\mathrm{Pe}\,\Sigma\int_{\delta_k}[N]^T[N]\{\omega^{(k)}\}[N](1+\{\Phi^{(k)}\}[N])\,d\delta_k,\ X,\ Y\in\Omega_a,$$

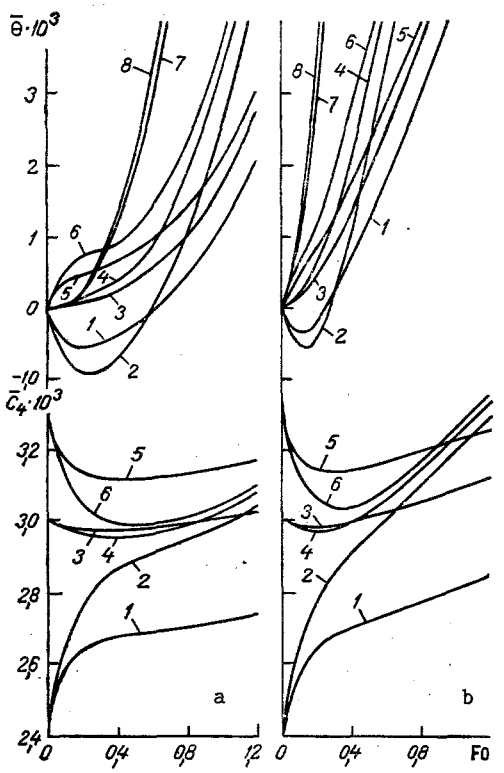

Fig. 2. Distribution of mean-mass flow temperature $\bar{\Theta}$ (1-6), average temperature $\bar{\Theta}_w$ (7, 8) about the perimeter of the fuel-shell surface, and mean-mass concentration $\bar{C}_4$ of oxygen in the mixture: a) linear release of heat; b) constant. T_0 = 500 K, P = 12 MPa: 1) C_{40}/C_{4equ} = 0.80, Z = 10; 2) 0.80 and 50; 3) 1.00 and 10; 4) 1.00 and 50; 5) 1.10 and 10; 6) 1.10 and 50; 7) 0.80 and 10; 8) C_{40}/C_{4equ} = 1.10; Z = 10.

$$[r_{1ij}] = \begin{cases} -K_\lambda \Sigma \int\limits_{\delta_k} [N]^T \left(\dfrac{\partial [N]^T}{\partial X} \dfrac{\partial [N]}{\partial X} + \dfrac{\partial [N]^T}{\partial Y} \dfrac{\partial [N]}{\partial Y} \right) d\delta_k, \; X, \; Y \in \Omega_c \cup \Omega_b, \\ -K_{\lambda a} \Sigma \int\limits_{\delta_k} [N]^T \left(\dfrac{\partial [N]^T}{\partial X} \left(\dfrac{\partial [N]}{\partial X} + [N]\{\Phi^{(k)}\} \, \mathrm{Le}_1 \dfrac{\partial [N]}{\partial X} \right) + \right. \\ \left. + \dfrac{\partial [N]^T}{\partial Y} \left(\dfrac{\partial [N]}{\partial Y} + [N]\{\Phi^{(k)}\} \, \mathrm{Le}_1 \dfrac{\partial [N]}{\partial Y} \right) \right) d\delta_k, \; X, \; Y \in \Omega_a, \end{cases}$$

$$\{g_{1i}\} = \begin{cases} \Sigma \int\limits_{\delta_k} [N]^T [N] \{q_c^{(k)}\} \, d\delta_k, \; X, \; Y \in \Omega_c, \\ 0, \quad X, \; Y \in \Omega_b, \\ -\Sigma \int\limits_{\delta_k} [N]^T [N] \{q_a'^{(k)}\} \, d\delta_k, \; X, \; Y \in \Omega_a, \end{cases}$$

$$[a_{2ij}] = K_{c\rho a} \Sigma \int\limits_{\delta_k} [N]^T [N] \, d\delta_k, \; X, \; Y \in \Omega_a,$$

$$[b_{2ij}] = K_{\lambda a} \, \mathrm{Pe} \, \Sigma \int\limits_{\delta_k} [N]^T [N] \{\omega^{(k)}\} [N] \, d\delta_k, \; X, \; Y \in \Omega_a,$$

$$[r_{2ij}] = -\mathrm{Le}_4 K_{\lambda a} \Sigma \int\limits_{\delta_k} [N]^T \left(\frac{\partial [N]^T}{\partial X} \frac{\partial [N]}{\partial X} + \frac{\partial [N]^T}{\partial Y} \frac{\partial [N]}{\partial Y} \right) d\delta_k, \quad X, \; Y \in \Omega_a,$$

$$\{g_{2i}\} = \Sigma \int\limits_{\delta_k} [N]^T [N] \{q_a''^{(k)}\} \, d\delta_k, \; X, \; Y \in \Omega_a.$$

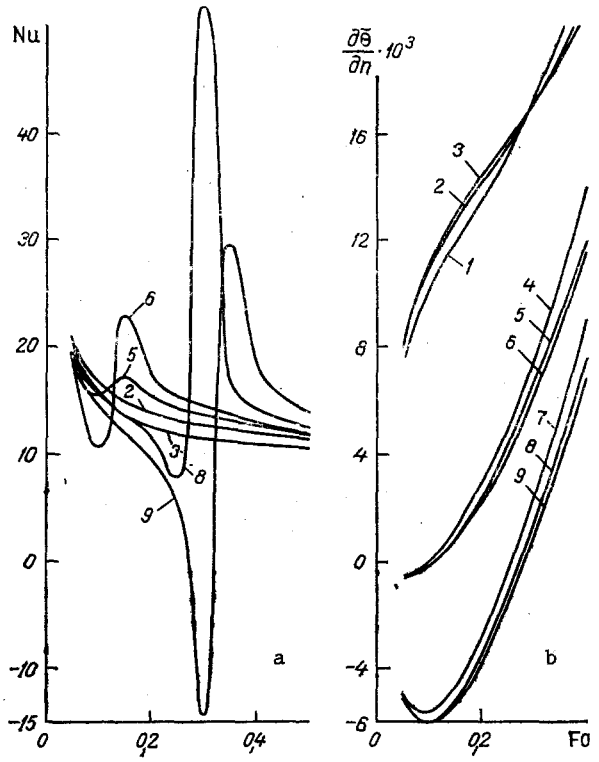

Fig. 3. Distribution of average heat flow about the shell perimeter $\bar{Q} = \partial\bar{\Theta}/\partial n$ (b) and of the Nusselt number $Nu = \bar{Q}/(\bar{\Theta}_w - \bar{\Theta})$ (a) for the linear heat-release regime. T_0 = 500 K, P = 12 MPa: 1) C_{40}/C_{4equ} = 0.80; Z = 10; 2) 0.80 and 20; 3) 0.80 and 50; 4) 1.00 and 10; 5) 1.00 and 20; 6) 1.00 and 50; 7) 1.10 and 10; 8) 1.10 and 20; 9) C_{40}/C_{4equ} = 1.10, Z = 50.

The solution of (17) is achieved by a grid method that is based on an unconditionally stable explicit-implicit running calculation scheme

$$[A_1]\frac{\{\vartheta\}_{j+1}^{i+1}-\{\vartheta\}_{j+1}^{i}}{\Delta Fo}+[B_1]\frac{\{\vartheta\}_{j+1}^{i+1}-\{\vartheta\}_{j}^{i+1}}{\Delta Z}=[R_1]\{\vartheta\}_{j+1}^{i+1}+\{G_1\}_{j+1}^{i+1}. \qquad (19)$$

This yields a system of nonlinear algebraic equations for the temperature values at the nodes of the fine elements of the calculation region at the instant of time (i + 1) and in that section of the channel along the axial coordinate with the number (j + 1), since the matrix in (17) and the load vectors in (17) and (18) are nonlinearly dependent on the values of the sought functions. The boundary conditions at the boundaries of the calculation region are satisfied automatically, while the adjoint conditions at the boundaries separating the media are achieved in the light of the very conception of the MFE.

In order to solve system (17) we use the Newton iteration method. The initial approximation is determined from the solution of this system for the matrices and the load vector, calculated from the values of the temperature and the concentration in the preceding time step by the Gauss method.

System of equations (18) is solved in analogous fashion.

As has been demonstrated by calculation, for purposes of determining the temperature fields and the concentrations at the (i + 1)-th instant of time and in the (j + 1)-th cross section of the channel along the axis it is convenient to use the following sequence of computations: 1) we solve the diffusion equation [the source term is calculated on the basis of the parameters from the i-th time interval and at the (j + 1)-th section of the channel]; 2) on the basis of the temperature from the i-th time step and the derived concentration we determine the matrices and the source term for the energy equation; 3) we solve the energy equation. The resulting fields of the sought functions are then used as the initial approximations for the further realization of the Newton method. After the calculation of the correc-

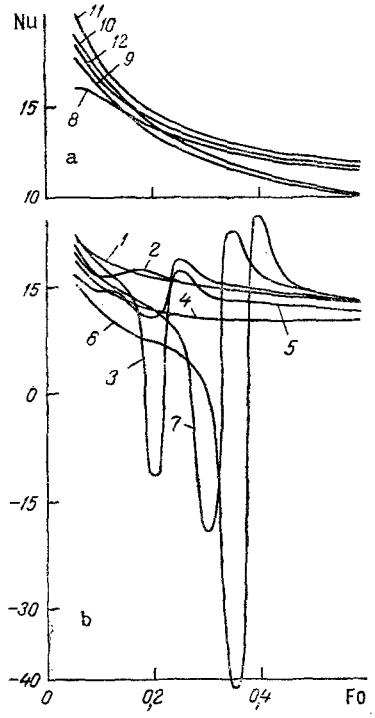

Fig. 4. Distribution of the Nusselt number Nu averaged over the shell perimeter for the linear heat-release regime (b) and a constant heat-release regime (a) as a function of the initial temperature and the inlet pressure: 1) C_{40}/C_{4equ} = 0.80, Z = 20, T_0 = 470 K, P = 12 MPa; 2) 1.00, 20, 470, and 12; 3) 1.24, 20, 470, and 12; 4) 0.80, 20, 530, and 12; 5) 1.00, 20, 530, and 12; 6) 1.05, 20, 530, and 12; 7) 1.12, 20, 500, and 14; 8) 1.10, 10, 500, and 12; 9) 1.10, 20, 500, and 12; 10) 1.10, 50, 500, and 12; 11) 0.80, 10, 500, and 12; 12) C_{40}/C_{4equ} = 1.00, Z = 10, T_0 = 500 K, P = 12 MPa.

tion factors the 1st iteration step is concluded. In the 2nd iteration step we determine (in the same sequence of calculations) the correction factors for the temperature fields and the concentrations from the 1st step, etc. The iteration process is brought to a conclusion as soon as the specified accuracy is attained.

Test calculations of the stationary heat and mass exchange in the case of the laminar flow of a nonequilibrium dissociating nitrogen dioxide in a circular tube under boundary conditions of the I-st kind, carried out to test the feasibility of the developed method, demonstrated its high efficiency and accuracy [8].

Below we present some of the results from our study of the effect of variable heat release in the cores of the fuel cells on the characteristics of the nonstationary heat and mass transport in a triangular cluster with a relative pitch of 1.1 [r_1 = 2.7 mm (UO_2), δ = 0.4 mm (Kh18N10T steel)] for two laws governing heat release, i.e., the linear (A) $q_V(\tau) = 0.8q_0\tau$ and the constant (B) $q_V(\tau) = q_0$ = const, where $q_0 = 0.75 \cdot 10^8$ W/m^3. The values of the initial oxygen concentration C_{40} in the flow were chosen to be smaller (I), equal to (II), and larger than (III) the equilibrium concentration C_{4equ}, determined from the condition of chemical equilibrium at the inlet temperature T_0 and the pressure P in the channel.

For each of the heat-release regimes with $C_{40} > C_{4equ}$ a drop in the mean-mass temperature of the mixture below the initial temperature is characteristic in the case of small Fo, which is a consequence of the predominance at this time of endothermic dissociation reactions in the flow (Fig. 2). As the oxygen content increases, the temperature begins to rise because of the reduction in the speed of the direct reactions, and because of the heating of the fuel cell. The distribution of the Nusselt number over time is monotonic in character (Fig. 3a and 4a). The mean-mass concentration of the oxygen in the mixture increases monotonically and at a maximum speed. When $C_{40} = C_{4equ}$ with a linear law governing the release of heat (the II-A regime) for Fourier numbers below 0.1 we observe a slight excess in the mean-mass

temperature $\bar{\Theta}$ of the flow over the fuel-cell surface temperature $\bar{\Theta}_w$ averaged over the perimeter (Fig. 2a). Moreover, the flows of heat at the surface of the shell at these instants of time are negative (Fig. 3b), since the temperature gradient at the surface of the fuel cell is directed into the stream. This leads to the appearance of oscillations in the distribution of the Nusselt number (Fig. 3a). The direct and reverse reactions proceed at speeds that are close to each other and C_4 therefore changes insignificantly, particularly in the II-A regime. The sharp intensification of these trends is found to occur as the initial oxygen concentration is elevated. Characteristic of the III-A regime is a substantial excess of $\bar{\Theta}$ above $\bar{\Theta}_w$, all the way to Fo = 0.25-0.3 (Fig. 2a), since the core of the fuel cell has not yet been significantly heated, while exothermic recombination reactions predominate within the gas mixture. The concentration of the oxygen diminishes rapidly, approaching equilibrium, and only after Fo = 0.4-0.5 does it begin to increase. The flows of heat at the fuel-cell surface attain minimum negative values (Fig. 3b). All of this leads to considerable oscillations of the distribution in the Nusselt number, in particular, the appearance of negative peaks (Fig. 3a and Fig. 4b). At the same time, when q_v = const the distribution of Nu is monotonic (Fig. 4a). The initial temperature T_0 and the inlet pressure P to the channel exert significant influence on the heat-exchange characteristics (Fig. 4b).

NOTATION

x, y, z, Cartesian coordinates, m; τ, time, sec; T, absolute temperature, K; ω_z, coolant flow velocity, m/sec; q_v, volumetric heat-release density in the fuel core, J/(m³·sec); $C_k = \rho_k/\rho$, mass fraction of the k-th component; ρ, density, kg/m³; c_p, isobaric heat capacity, J/(kg·K); λ, thermal conductivity, W/(m·K); μ, dynamic viscosity, kg/(m·sec); D_k, effective coefficient of the diffusion of the k-th component, m²/sec; m_k, molecular mass of the k-th component; m, molecular mass of the mixture; J_4, source (flow) of the mass of oxygen as a result of the reaction, kg/(m³·sec); K_{npII}, NO_2 dissociation rate constant, cm³/(mole·sec); ΔH_pI, ΔH_pII and K_{cI}, K_{cII}, thermal effect, J/mole, and equilibrium constants of the Ist and IInd stages of the nitrogen tetroxide dissociation reaction; R, universal gas constant, J/(kmole·K); Pe, Le_1, Le_4, Peclet and Lewis numbers; $\Theta = (T - T_0)/T_0$, dimensionless temperature; $C = C_4 - C_{40}$, reduced concentration of O_2; $\Phi = c_{pr}/c_{pf}$; $Q_a' = (\varphi_1\Delta H_{p1} + \Delta H_{pII})J_4 d_e^2/m_4\lambda_b T_0$; $Q_a'' = J_4 c_{pf} d_e^2/\lambda_b$; $Q_c = q_v d_e^2/\lambda_b T_0$; $K_{c\rho i} = c_{pi}\rho_i/c_{pb}\rho_b$; $K_{\lambda i} = \lambda_i/\lambda_b$, i = a, b, c; $W = \omega_z/\omega$; ω, mean mass flow rate, m/sec; $X = x/d_e$; $Y = y/d_e$, $Z = z/d_e$, dimensionless coordinates; $Fo = \lambda_b\tau/c_{pb}\rho_b d_e^2$, Fourier number; d_e, equivalent channel diameter, m; K_Φ, channel form factor. Subscripts: f, "frozen in" component; r, reaction component; 0, initial value; a, b, c, parameters of the coolant, the shell, and the fuel core; 1) N_2O_4; 2) NO_2; 3) NO; 4) O_2; I, first reaction stage; II, second stage.

LITERATURE CITED

1. V. B. Nesterenko and B. E. Tverkovkin, The Exchange of Heat in Nuclear Reactors with a Dissociating Heat-Carrying Coolant [in Russian], Minsk (1980).
2. L. I. Kolykhan and B. V. Nesterenko, Heat Exchange in a Dissociating Nitrogen Tetroxide Coolant [in Russian], Minsk (1977).
3. A. E. Kuznetsov, O. A. Nekhamkina, and M. Kh. Strelets, Experimental and Theoretical Studies of the Transfer of Heat and Mass in the Flow of Dissociating Gases in Channels. Collection of Scientific Papers, IYaÉ, Akad. Nauk BSSR [in Russian], Minsk (1983), pp. 48-57.
4. A. A. Mikhalevich, V. I. Nikolaev, V. A. Nemtsev, and L. N. Shegidevich, in: Heat and Mass Exchange 7: Materials of the 7th All-Union Conference on Heat and Mass Exchange, Minsk, May, 1984, Vol. 3, pp. 134-139.
5. V. V. Lapin, A. A. Ryadno, and A. P. Yakushev, Vestsi Akad. Navuk BSSR, Ser. Fiz.-Énerg., Navuk, No. 3, 94-97 (1986).
6. A. N. Devoino and S. V. Chernousov, Vestsi Akad. Navuk BSSR, Ser. Fiz.-Énerg. Navuk, No. 4, 32-36 (1984).
7. G. A. Sharovarov, The Physics of Nonstationary Nuclear Power Plant Processes [in Russian], Minsk (1985).
8. V. V. Lapin, A. A. Kochubei, and A. A. Ryadno, Mathematical Methods in Heat and Mass Transfer. Collection of Scientific Papers, Dnepropetrovsk State University (1984), pp. 62-68.